SolarPACES 2022, 28th International Conference on Concentrating Solar Power and Chemical Energy Systems
Receivers and Heat Transfer Media and Transport: Point Focus Systems
https://doi.org/10.52825/solarpaces.v1i.717

Published: 05 Jan 2024

Particle Flow Distribution in a Fluidized-Particles Multitube Solar Receiver

Guillaume Sahuquet[1][https://orcid.org/0000-0003-0275-2890], Ronny Gueguen[1][https://orcid.org/0000-0002-5236-8638] Lilian Fontalvo[2], Samuel Mer[3,a][https://orcid.org/0000-0001-7915-3146], Adrien Toutant[3,a][https://orcid.org/0000-0002-7156-1732], Françoise Bataille[3,b][https://orcid.org/0000-0003-4470-8636], and Gilles Flamant[4][https://orcid.org/0000-0003-4562-8515]

[1] PROMES-CNRS, UPVD, 7 rue du Four Solaire, 66120 Odeillo, France.

[3] PROMES-CNRS, UPVD, Rambla de la Thermodynamique, Tecnosud, 66100 Perpignan, France

[4] PROMES-CNRS (UPR 8521), 7 rue du Four Solaire, 66120 Odeillo, France.
Corresponding author: +33(0) 4 68 30 77 00, Gilles.Flamant@promes.cnrs.fr

Abstract. A fluidized-particles two-tube solar receiver was tested at ambient temperature at PROMES Laboratory to investigate the influence of an inhomogeneous solar flux density on the particle mass flow rate between the tubes. The principle of this 3rd generation solar receiver is to fluidize the particles in a container, called dispenser, in which the tubes' bottom are immersed. The fluidized particles are flowing upward the tubes by applying an overpressure in the dispenser. Air velocities are changed inside the tubes, thanks to air mass flow controllers, to represent temperature heterogeneity between the tubes. Air velocities from 0.05 up to 0.52 m/s were tested, both in homogeneous and heterogeneous conditions. In the heterogeneous ones, the differences in air velocity between the tubes aim to mimic a difference in temperature from 20 to 100 % with homogeneous air flow rates injected. The following conclusions were drawn. First, the particle mass flux in the tubes are the same with homogeneous air velocities, each one following a calibration map previously obtained. Second, different air velocities lead to different particle mass flux. Third, the rise of the total particle mass flux diminishes the pressure in the dispenser. Four, this diminution of pressure leads to a decrease of the particle mass flow rate of the tube with the lower air velocity. This influence can lead in some cases to the stop of the fluidized bed circulation in the affected tube.

Keywords: Concentrated Solar Power, Particles Solar Receiver, Fluidized Particles, Particle Flow Heterogeneity in Solar Receiver.

Introduction

Concentrated Solar Technologies consist of concentrating solar irradiation thanks to mirrors onto a receiver in order to produce heat. A heat transfer fluid (HTF) absorbs and conveys the thermal energy that can be stored or used to heat a working fluid in a heat exchanger. The working fluid is coupled with a thermodynamic cycle that converts heat into electricity. The cycle conversion efficiency depends on the temperature of the heat source, according to the Carnot's principle. Nowadays, molten salts are commonly used as HTF in power towers [1] and have a limited operating temperatures in the range 220-565 °C that limits the efficiency of the power block to ~42 % [2].

To overcome these issues and improve the conversion efficiency from 42 to 50 %,

new HTF and high efficiency cycles are developed. Supercritical cycles need temperature between 600 °C and 750 °C. Among possible new HTF, solid particles can withstand temperature up to 1400 °C, while reducing drastically storage cost. New particle receivers are under development worldwide [3] as the falling particle receiver of Sandia National Laboratories [4], the centrifugal receiver of the German Aerospace Center [5] and the fluidized particle-in-tube of the French National Center for Scientific Research (CNRS-PROMES Laboratory) [6].

The latter has already been demonstrated and an extensive experimental data base was established thanks to several projects, either at ambient temperature [7,8] or under concentrated solar flux [9-12]. In particular, tests at large scale with forty 3 m-long tubes under concentrated solar irradiation of the Horizon2020 Next-CSP project [13] revealed the existence of heterogeneity in particle mass flow rate among the tubes. One of the possible explanations is a difference in air velocity between tubes due to temperature heterogeneity. To reproduce this phenomenon, a 2-tube cold mock-up was built at PROMES Laboratory. Changing the aeration velocity in each tube aims to reproduce the difference of air velocity due to temperature heterogeneity between tubes. This protocol mimics the effect of temperature but still neglect the air viscosity effect.

Experimental Setup

The cold mock-up is composed of two 3.70 m-long glass tubes of 45 mm internal diameter. Figure 1 shows a 3D (a) and a schematic representation (b) of the cold mock-up. The particles used are 61 µm Sauter diameter olivine belonging to the group A of Geldart classification [14]. They are fluidized in a container, called “dispenser“, thanks to a homogeneously distributed air flow rate (qf) of 16.7 sm3/h (corresponding to 2.4 times the minimum fluidization velocity). By applying an overpressure in the freeboard of the dispenser with a pressure-control valve, the fluidized bed flows upwards inside the two tubes and particles are collected in weighting devices to measure the particle mass flux (GP) in each tube, varying from 0 to 260 kg/(m².s) (i.e. 1470 kg/h).

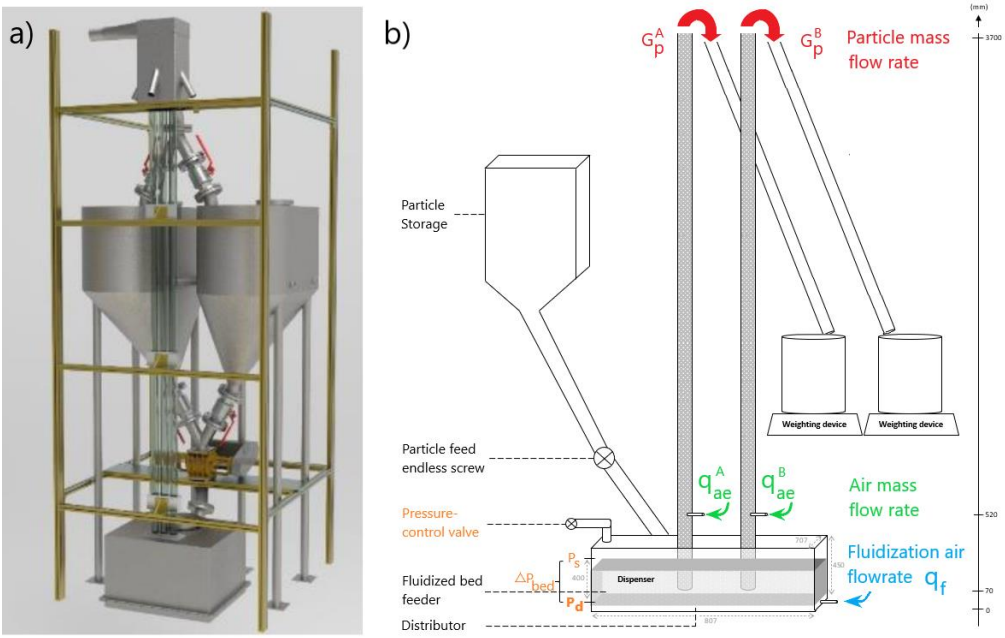

Figure 1. a) 3D and b) schematic representation of the 2-tubes experimental setup.

In the 2-tube mock-up, the air velocity in each tube varies thanks to air mass flow controllers connected to injection nozzles located at 52 cm above the bottom of the tubes. The air flow rate can vary from 0 up to 2.50 sm^3/h (superficial air velocity inside the tubes from 0 up to 0.52 m/s). Injection nozzles are part of the fluidized particle-in-tube technology

aiming at stabilizing the particle flow and controlling the fluidization regime. The particle volume fraction and the fluidization regime inside a tube are directly related to the air velocity [7]. The tube close to the pressure-control valve is named Tube A and the other one, Tube B. When particles flow out of the tube, an endless screw connected to a particle storage is activated to compensate the loss of particles in the dispenser.

A previous study with the same configuration but with a single tube resulted in the calibration map represented in Figure 2 [8]. This map is a plot of the particle mass flux (Gp) versus the pressure imposed at the bottom of the dispenser. The latter is the sum of the freeboard pressure and the pressure drop through the fluidized bed, of ~20–40 mbar over all the tests. Each color corresponds to a given aeration air flow rate.

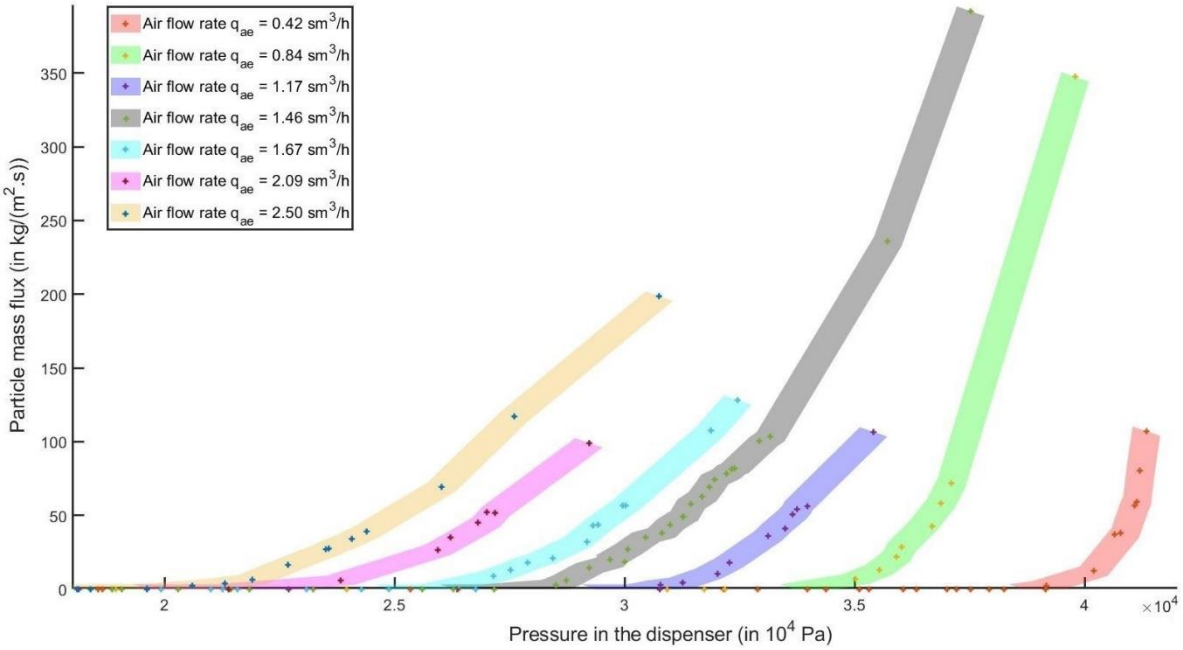

Figure 2. Particle mass flux (in kg/(m².s)) for one tube as a function of the pressure at the bottom of the dispenser (in Pa) and the air flow rate (in sm3/h).

Both a given pressure in the freeboard of the dispenser (in the x-axis) and a given air flow rate (in color) result in a particle mass flux (in y-axis) circulation inside the tube. The variation of these parameters enables to plot the colored zones with uncertainties taken into account. The latter are due to the pressure sensors and the weighing scale accuracies. We observed that this map is valid for 1, 2 and 3 tubes configurations. Although some experiments were carried out with three tubes, results of test with two tubes are reported in this paper since no significant differences have been observed between two and three tubes.

Results and discussion

The operating procedure is the following:

- Progressive homogeneous increase of air flow rates injected inside the tubes (Fig.3.a) through the injection nozzles that creates, with the appropriate initial pressure in the freeboard of the dispenser, particle mass fluxes in the 2 tubes (Fig.3.b) (time intervals 1-3).

- Then, only the air flow rate of tube A is changed to a higher value, triggering a rise in the particle mass flux through it (time intervals 4 and 5). The particle feeding of the dispenser is changed to keep the mass of particle in the dispenser constant.

Time intervals are 3 minutes long and the particle and air flow rates are averaged on the last minute of each interval to take into account the stationary state and not the transient part.

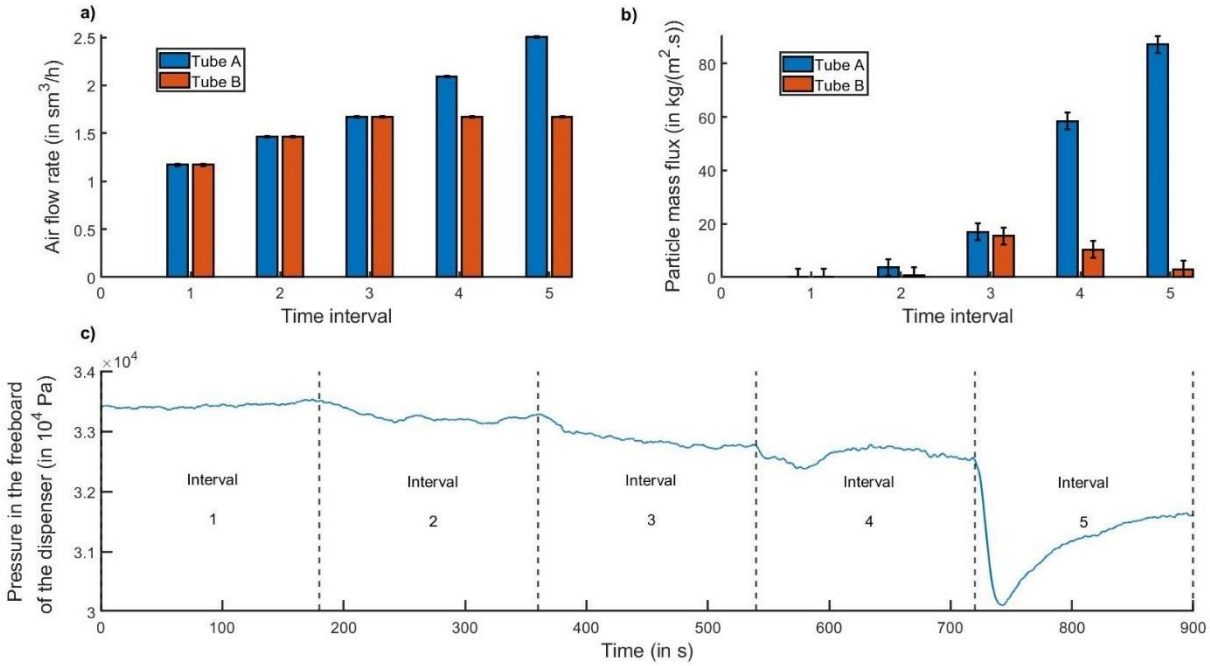

Figure 3. Experimental test 1 - a) Air flow rate (in sm3/h) and b) particle mass flux (in kg/(m².s)) for tube A (in blue) and B (in orange) for different time intervals. c) Pressure in the freeboard of the dispenser (in Pa) through time (in s).

Seven experimental tests were conducted, for initial pressure in the freeboard of the dispenser between 269 and 413 mbar and initial air flow rates between 0.25 and 1.17 sm3/h. The same procedure is followed for each test with three time intervals of increasing homogeneous air velocities (same air flow rate injected in the two tubes) followed by 2 time intervals of heterogeneous air flow rates (different air flow rates injected in the two tubes) configurations. These heterogeneous air flow rates configurations aim to reproduce homogeneous air flow rates configurations with heterogeneous temperatures (with Tube A temperature in K from 1.2 to 2 times higher than Tube B).

Several observations can be drawn. Firstly, for the homogeneous aeration configurations:

1. The tubes experience the same particle mass flux when the same air flow rate is injected in each tube. In addition, the particle flux inside each tube follows the calibration map in Figure 2.
2. Increasing the air velocity results in a decrease of the particle volume fraction and in the dilution of the mixture. This variation leads to an increase of the particle mass flux since the pressure drop created by the fluidized bed decreases (it is proportional to the particle volume fraction) [8].
3. The increase of the total particle mass flux results in a decreases of the pressure in the freeboard of the dispenser. (Fig.3.c).

Secondly, for the heterogeneous aeration configurations:

1. The effect of the diminution of the dispenser freeboard pressure induced by the increase of the total particle mass flux is strongly correlated to the decrease of the particle mass flux in tube B. This decrease can be extended until a threshold value of air velocity in the tube A for which the particle mass flux in the other tube becomes null.
2. The higher the total particle mass flux (sum of Tubes A and B), the higher the decrease in pressure in the freeboard of the dispenser, even in heterogeneous aeration configuration. Figure 4 plots the resulting linear correlation between the particle mass flux and the pressure decrease in the dispenser freeboard. An explanation is yet to be developed.

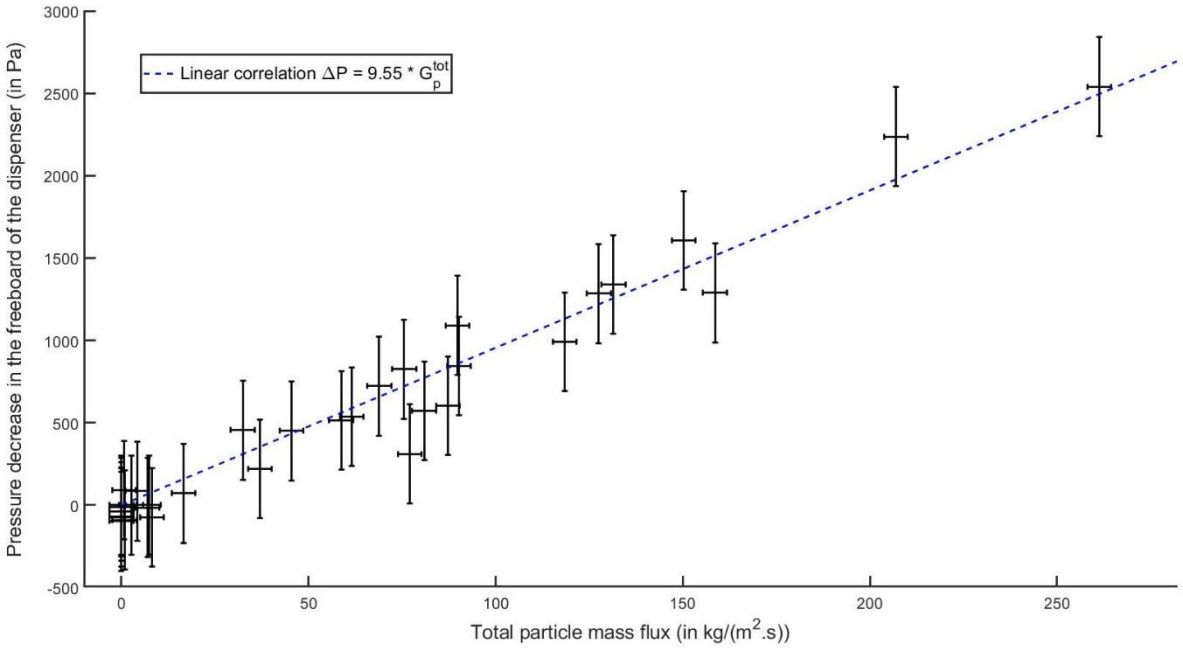

Figure 4. Decrease of the pressure in the freeboard of the dispenser (in Pa) as a function of the total particle mass flux (in kg/(m².s)).

Figure 5 illustrates the evolution path of the particle mass flux inside tube A and tube B due to the variations of the aeration air flow rate. The experimental results are plotted in the calibration map to emphasize dynamically the evolution of the particle mass flux inside each tube. Only experiments 1, 2 and 5 are represented among the total of the seven conducted tests to facilitate the reading. Test 1 corresponds to the test described previously in Figure 3 with the associated interval numbers.

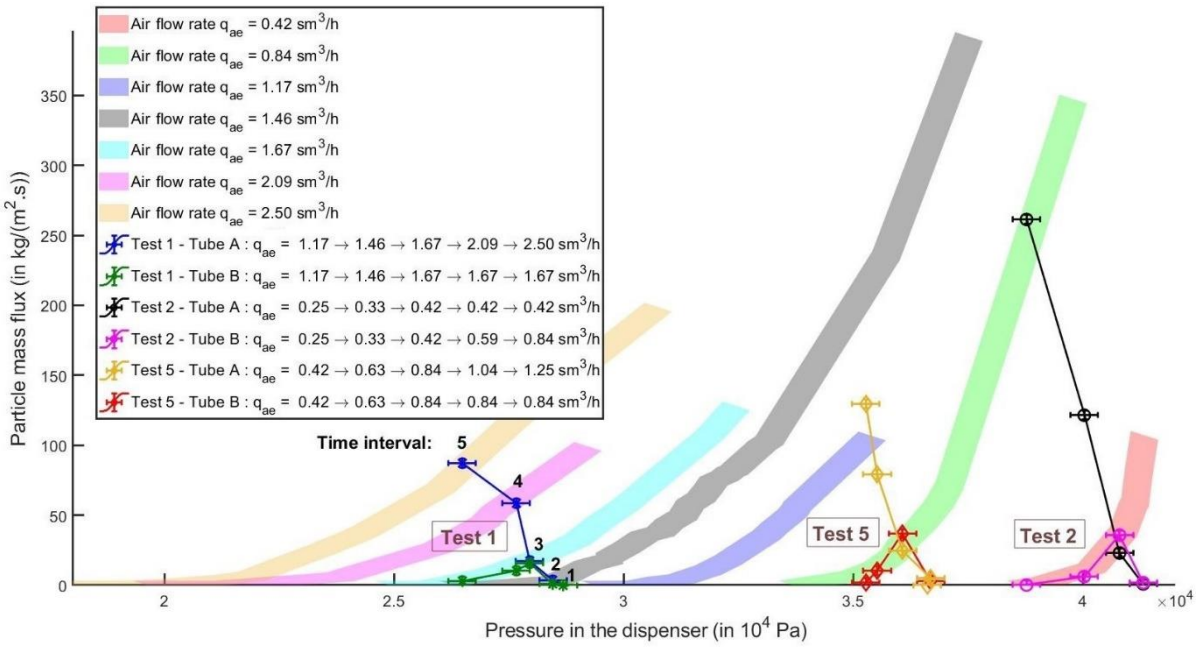

Figure 5. Results of experimental tests 1, 2 and 5 represented in the calibration map of the system.

This representation clearly shows that as the total particle mass flux increases, the pressure in the freeboard of the dispenser decreases, as the points are all left shifted. Let us comment results of test 1, represented by the left blue (Tube A) and green (Tube B) curves. Time intervals are denoted by black numbers. At the third time interval of test 1, the particle mass flux and the pressure in the dispenser are in the blue zone corresponding to the calibration zone of an air flow rate injected of 1.67 sm^3/h in both tubes. For time intervals 4 and 5, air flow rate of tube A rises and the associated particle mass flux fits with the corresponding air flow rates of respectively 2.00 and 2.50 sm^3/h, i.e. pink and yellow zones. Meanwhile, air flow rate in tube B is kept constant and, consequently, the associated particle mass flux follows the blue zone downward as the pressure decreases. For test 2 with the rightmost curves, the particle mass flux of tube B (in dark pink) reaches zero at time interval 5, in other words the fluidized bed stopped circulating through it.

Conclusion

A cold mock-up that can receive one, two or three tubes was built at PROMES Laboratory in order to understand phenomena observed at the pilot-scale fluidized-bed solar receiver of the Next-CSP project that is composed of 40 tubes, 3 m long (irradiated zone). In some operation conditions, we observed that particle circulation flux strongly reduces inside some of the tubes. The main hypothesis is that an inhomogeneous solar flux distribution onto the tubes creates temperature differences among the tubes resulting in air velocity differences inside the tubes. To represent this phenomenon, inhomogeneous air flow rates are injected in the tubes of the cold mock-up. The particle mass flux and the related pressure in the freeboard of the dispenser are studied. It is shown that particle circulation can stop inside the tube where low aeration flow rate is maintained.

Further work, both experimental and theoretical, is currently ongoing in order to better understand the phenomena at stake. Nonetheless, one can draw the following conclusions:

1. For each tube, a given pressure in the freeboard of the dispenser and the same air flow rate result in the same particle mass flux flowing inside both tubes. This characteristic enables plotting a particle mass flux calibration map.
2. Upon the hypothesis that a heterogeneous solar flux distribution leads to inhomogeneous air temperature among the tubes, air velocities are heterogeneous and so the particle mass flux.
3. The pressure in the dispenser is influenced by the total particle mass flux. When the latter increases, the former decreases linearly, and vice versa.
4. The particle circulation inside the tubes is influenced by the pressure diminution and the resulting particle mass flux diminishes following the curves corresponding to the air flow rate in the calibration map.
5. For heterogeneous air flow rate aeration configurations, the tube with the lower air velocity experiences a strong diminution in the particle mass flux, that can lead in some cases to the stop of the fluidized bed circulation.

Current experimental tests under concentrated solar flux at the Odeillo's 1MW solar furnace (France) show that the previous effects would be reduced by the variation of temperature created by the change in particle mass flux. This positive feedback can be explained as follows. Indeed, if the particle mass flow rate decreases in a tube, the thermal power extracted also decreases and thus the particle and air temperature increase, and the air velocity too, resulting in an increase of the particle mass flow rate. We observed this autoregulation phenomenon for both low and high air flow rates.

Data availability statement

The data supporting the results can be accessed asking the authors.

Author contributions

Conceptualization, supervision, and resources, G.F.; methodology, software and investigation, G.S. and R.G.; validation and formal analysis, S.M., A.T., F.B. and G.F.; data curation, G.S., L.F. and R.G.; writing—original draft preparation, G.S. and R.G.; writing—review and editing, R.G., S.M., A.T., F.B. and G.F.; funding acquisition, G.F. All authors have read and agreed to the published version of the manuscript.

Competing interests

The authors declare no competing interests.

Funding

This work was funded by the French "Investments for the future" ("*Investissements d'Avenir*") programme managed by the National Agency for Research (ANR) under contract ANR-10-LABX-22-01 (labex SOLSTICE) and the U.S. Department of Energy, Solar Energy Technologies Office under Award Number 34211. Additional funding was awarded by the European Union's Horizon 2020 research and innovation program under Grant Agreement 727762, Next-CSP project and by the Occitanie French region for the cold mock-up facility.

Acknowledgement

Authors thank Jean-Yves Peroy for the design of the experimental test bench.

References

1. Md. T. Islam, N. Huda, A.B. Abdullah, R. Saidur, “A comprehensive review of state-of-the-art concentrating solar power (CSP) technologies: Current status and research trends“, Renew. Sustain. Energy Rev, vol.91, pp. 987-1018, 2018, https://doi.org/10.1016/j.rser.2018.04.097.
2. H. Benoit, L. Spreafico, D. Gauthier, G. Flamant, “Review of heat transfer fluids in tube-receivers used in concentrating solar thermal systems: Properties and heat transfer coefficients“, Renew. Sustain. Energy Rev, vol.55, pp.298-315, 2016, https://doi.org/10.1016/j.rser.2015.10.059.
3. C. K. Ho, “A review of high-temperature particle receivers for concentrating solar power“, Applied Thermal Engineering, vol.109, pp. 958-969, 2016, https://doi.org/10.1016/j.applthermaleng.2016.04.103.
4. C. K. Ho, J. Christian, J. Yellowhair, S. Jeter, M. Golob, C. Nguyen, K. Repole, S. Abdel-Khalik, N. Siegel, H. Al-Ansary, A. El-Leathy, B. Gobereit, “Highlights of the high-temperature falling particle receiver project: 2012-2016”, AIP Conference Proceeding, 1850, 030027, 2017, https://doi.org/10.1063/1.4984370.
5. W. Wu, L. Ambseck, R. Buck, R. Uhlig, R. Ritz-Paal, “Proof of concept test of a centrifugal particle receiver”, Energy Procedia, vol.49, pp. 560–568, 2014, https://doi.org/10.1016/j.egypro.2014.03.060.
6. O. Behar, B. Grange, G. Flamant, “Design and performance of a modular combined cycle solar power plant using the fluidized particle solar receiver technology“, Energy Convers. Manag., vol.220, 113108, 2020, https://doi.org/10.1016/j.enconman.2020.113108.
7. R. Gueguen, G. Sahuquet, S. Mer, A. Toutant, F. Bataille, G. Flamant, “Gas-Solid Flow in a Fluidized-Particle Tubular Solar Receiver: Off-Sun Experimental Flow Regimes Characterization“, Energies, vol.14, pp. 7392, 2021 https://doi.org/10.3390/en14217392.
8. R. Gueguen, G. Sahuquet, S. Mer, A. Toutant, F. Bataille, G. Flamant, “Fluidization Regimes of Dense Suspensions of Geldart Group A Fluidized Particles in a High Aspect Ratio Column”, Chemical Engineering Science, 118360, 2022, doi: https://doi.org/10.1016/j.ces.2022.118360.
9. A. Le Gal, B. Grange, M. Tessonneaud, A. Perez, C. Escape, J.L. Sans, G. Flamant, “Thermal analysis of fluidized particle flows in a finned tube solar receiver“, Sol. Energy, vol.191, pp. 19-33, 2019, https://doi.org/10.1016/j.solener.2019.08.062.
10. H. Benoit, I. Perez Lopez, D. Gauthier, J.-L. Sans, G. Flamant, “On-sun demonstration of a 750 °C heat transfer fluid for con-centrating solar systems: Dense particle suspension in tube“, Sol. Energy, vol.118, pp. 622–633, 2015, https://doi.org/10.1016/j.solener.2015.06.007.
11. I. Perez-Lopez, H. Benoit, D. Gauthier, J.-L Sans, E. Guillot, G. Mazza, G. Flamant, “On-sun operation of a 150 kWth pilot solar receiver using dense particle suspension as heat transfer fluid“. Sol. Energy, vol.137, pp. 463–476, 2016, https://doi.org/10.1016/j.solener.2016.08.034.
12. B. Boissière, R. Ansart, D. Gauthier, G. Flamant, M. Hemati, “Experimental Hydrodynamic Study of Gas-Particle Dense Sus-pension Upward Flow for Application as New Heat Transfer and Storage Fluid“, Can. J. Chem. Eng., vol.93, pp. 1–14, 2015, https://doi.org/10.1002/cjce.22087.
13. Next-CSP project. 2020. High Temperature Concentrated Solar Thermal Power Plant with Particle Receiver and Direct Thermal Storage. Available online: http://cordis.europa.eu/project/id/727762 (accessed on August 17 2022).
14. D. Geldart, “Types of Gas Fluidization”, Powder Technology, vol.7, pp. 285–292, 1973, https://doi.org/10.1016/0032-5910(73)80037-3.